IEEE Access
Multidisciplinary | Rapid Review | Open Access Journal

Received February 9, 2020, accepted March 7, 2020, date of current version March 19, 2020.

Digital Object Identifier 10.1109/ACCESS.2020.2980242

Cooperative Jamming for Secure UAV-Enabled Mobile Relay System

JIANSONG MIAO AND ZIYUAN ZHENG
Beijing Laboratory of Advanced Information Networks, Beijing University of Posts and Telecommunications, Beijing 100876, China
Corresponding author: Ziyuan Zheng (ziyuanzheng@bupt.edu.cn)

This work was supported in part by the Beijing Municipal Natural Science Foundation under Grant 19L2034.

ABSTRACT Due to the air-to-ground line-of-sight communication links, it is challenging to deal with the security threats in the wireless system with unmanned aerial vehicles (UAVs) integrated. In a UAV-enabled mobile relay system, the paper proposes a novel cooperative communication scheme from a physical layer security perspective to address the security issue. Specifically, in a mobile relay system where a UAV relay is employed to forward confidential information between two ground users, an eavesdropper exists on the ground wiretapping the relay UAV. To enhance the security performance of the system, we introduce a friendly UAV jammer transmitting interference signals and confusing the eavesdropper. A secrecy rate maximization problem is then formulated, subject to mobility constraints, power constraints on both UAVs and the information-causality constraint on the relay UAV. To solve the non-convex optimization problem with closely coupled variables, we decouple the problem into more tractable subproblems. An iterative algorithm is thus proposed to optimize the transmit power and flight trajectory of both UAVs alternately via the update-rate-assisted block coordinate descent and successive convex approximation techniques. Simulation results demonstrate that proposed cooperative design can significantly improve the secrecy rate of the UAV-enabled mobile relay system compared to benchmark schemes.

INDEX TERMS Cooperative communication, mobile relaying, physical layer security, UAV communication.

I. INTRODUCTION

Unmanned aerial vehicles (UAVs) have the characteristics of high mobility and line-of-sight (LoS) dominated UAV-ground communication links. Compared to a simple terrestrial wireless system, UAVs can be deployed rapidly in a wireless communication system to obtain better flexibility and a higher achievable rate. Thanks to the advantages mentioned above and the gradually decreasing cost of the UAV, UAV-enabled communication systems have gained increasing interest in recent years. Moreover, with the evolution of the 5G standard, the non-terrestrial network (NTN) will be the next hot spot in the future, where UAVs will continue to play an essential role in providing ubiquitous access. Much research has been conducted on the UAV-enabled communication system. UAVs can serve as stationary aerial base stations to maximize the coverage for ground terminals [1]. The work in [2]–[4] consider UAV-ground downlink communication. Y. Zeng *et al.* study UAV's energy-efficient communication and flight strategy [2]. A multi-UAV network is presented in [3], where all UAVs serve as information sources. Instead of throughput maximization, the goal in [4] is minimizing the mission completion time of the UAV in a multicasting system. In [5]–[8], UAVs are employed as mobile relays in a communication system where the terrestrial channels suffer severe blockage. Zhang *et al.* propose an iterative algorithm to maximize throughput in a UAV-enabled mobile relay system via successive convex approximation and block coordinate descent techniques [5]. The work in [6] studies the optimum placement of a relay UAV to enhance reliability. Joint trajectory and power optimization is performed in a UAV relay network [7] to minimize the system outage probability. Multi-UAV relay system is studied in [8] considering two cases: a single multi-hop link and multiple dual-hop links. Other applications of UAV in communication contain IoT-enabled UAV [9], UAV-assisted backhaul in mmWave cellular networks [10], communications between cellular UAV and base

The associate editor coordinating the review of this manuscript and approving it for publication was Mostafa Zaman Chowdhury.

station [11] and UAV-enabled data collection in wireless sensor network [12].

However, the physical layer security problem in the UAV-integrated wireless communications system needs to be solved due to the broadcast and shared nature of wireless channels. The dominated line-of-sight link in the UAV-to-ground channel makes the security problem even more severe. From a physical layer security perspective, security threats in the wireless system with UAV integrated can be divided into two main scenarios [13]. On the one hand, UAV-ground communications are more prone than terrestrial communications to eavesdropping and jamming attacks by malicious nodes on the ground, and the corresponding problem is denoted by securing legitimate UAV communications in the wireless network. On the other hand, compared to malicious ground nodes, malicious UAVs can launch more effective eavesdropping and jamming attacks to terrestrial communications, which is denoted by safeguarding terrestrial networks against malicious UAV attacks. By jointly optimizing trajectory and transmit power of the UAV, [14] maximizes average achievable secrecy rate in a single-UAV single-user broadcast system with a ground eavesdropper. A three-terminal ground wiretap system is considered in [15], where a jammer UAV is introduced to transmit jamming signals to the eavesdropper cooperatively. In [16], serving as a base station and a jammer, respectively, two UAVs are deployed cooperatively with multiple information receivers and multiple eavesdroppers. The trajectory and transmit power of both UAVs are jointly optimized to maximize the minimum average secrecy rate over all information receivers (IRs), which ensures fairness among ground terminals. A similar problem is formulated under partial eavesdropper information in the scenario where a single UAV still serves as a mobile base station [17]. In [18], two UAVs are employed as an information source and a friendly jammer, respectively, with multiple ground eavesdroppers. The trajectory and power for both UAVs are jointly optimized to maximize the worst-case secrecy rate of the system.

References [13]–[18] discuss the physical layer security issue in their model where the UAVs are commonly used as base stations. However, the mobile relay is another important application for UAVs in UAV-enabled communication systems [5]–[8]. The physical layer seissuescurity problem in UAV-enabled relay systems is also urgent to be solved. However, the UAV relay systems mentioned in previous literature [5]–[8] do not consider security issues. In [19], a ground eavesdropper exists in the UAV mobile relaying system, but the scheme in [19] only performs trajectory optimization for a single relay UAV. The work in [20] jointly optimized trajectory and power for a UAV relay. However, the model still stays in the scene of a single relay UAV without introducing the idea of cooperative communication.

To fill the vacancy in the research on the secure UAV-enabled mobile relay system, we propose a novel scheme where two UAVs are cooperatively deployed to improve the security performance of the UAV-enabled relay communication system with a ground eavesdropper. In our proposed scheme, the ground communication links suffer severe blockage due to mountains, jungles, or other harsh communication environments. One of the UAVs serves as a mobile relay to enable the communication between a source user and a destination user. An illegal eavesdropper on the ground wiretaps the information forwarded by the UAV relay. There is another UAV serving as a friendly jammer and transmitting jamming signals to confuse the ground eavesdropper. Our goal is maximizing the average achievable secrecy rate in the UAV-enabled mobile relay system. In the cooperative secure mobile relaying scheme, the data received by the relay UAV from the information source need to be temporarily stored in a buffer before being forwarded to the destination to exploit the movement-induced channel variations [5]. However, unlike some literature studying the strategy on the buffer-aided relay [21], we focus on investigating the cooperative communication scheme by utilizing the resources on the UAVs, which include flight trajectory and transmit power. We therefore formulate a simple but practical relay buffer model, where the relay can only forward the data that has been previously received from the source. In the problem formulation, the relay buffer model is presented by the *information-causality constraint* [5]. In the UAV-enabled mobile relaying systems, the data may need to be buffered for a longer duration for the relay to reach a better position for information forwarding. Though a larger delay may have to be tolerated by some of the packets transmitted, mobile relaying with optimally designed power allocation and UAVs' trajectory is able to achieve significant secrecy rate gains [5]. Besides, [22] points out that UAV's movement may consume much propulsion energy of the UAV, which leads to a new fundamental energy tradeoff in UAV-ground wireless communication. The cooperative secure relay enabled by the jammer UAV and relay UAV consumes more propulsion energy than single UAV schemes. In our present paper, we investigate the proposed cooperative jamming scheme in a mobile relay system to improve the security performance and draw insights from the novel scheme, which brings significant secure performance gains over single UAV schemes.

Then, we propose an effective algorithm to jointly optimize the flight trajectory and transmit power for both UAVs (i.e., the relay UAV and the jammer UAV) iteratively in an alternating manner. The main contributions of this paper are summarized as follows:

- This paper presents a novel cooperative design to improve the physical layer security performance of the UAV-enabled mobile relaying in a wireless communication system. In our proposed scheme, two UAVs are employed with given maximum speed as well as initial and final locations. The relay UAV enables the communication between source and destination while another UAV serving as friendly jammer confuses the eavesdropper. We formulate an average achievable secrecy rate maximization problem with joint optimization on both UAVs' trajectory and transmit power over all time

slots, subject to mobility constraints, transmit power constraints, and the information-causality constraint.

- The original problem is non-convex with closely coupled optimization variables. To handle the complicated non-convex problem, we decouple the original problem into four subproblems. However, the subproblems with the information-causality constraint are still non-convex. Thus, the successive convex approximation technique is applied to transform the subproblems into more tractable and convex forms, respectively, which optimize the lower bound of the original subproblems. With the solutions to the subproblems, we utilize update-rate-assisted block coordinate descent method to solve the subproblems iteratively in an alternating manner until the increment of the average achievable secrecy rate is below a threshold.
- The effectiveness of our proposed cooperatively joint trajectory and power optimization scheme (denoted by C-T&P in later sections) is validated by simulations. Compared with three benchmark schemes in two cases under different flight periods, our proposed scheme obtains a significant and stable performance improvement.

It is worth noting that there have been prior works (e.g. [14]) on physical layer security in the UAV communication system. The work in [14] is introduced in the literature review. Although our proposed scheme is partially enlightened by [14], we propose a novel *cooperative jamming scheme* in the UAV-enabled *mobile relay system* from a cooperative communication perspective. In our paper, different from the single-user single-UAV model in [14], the UAV-enabled mobile relay system with the *information-causality* constraint is investigated. From a cooperation perspective, we also introduce a friendly jammer to cooperatively enable secure mobile relaying, which serves as a fundamental difference from [14].

The rest of this paper is organized as follows. Section II introduces the system model and presents the problem formulation for secrecy rate maximization. In Section III, we decouple the original problems into four subproblems and solve them respectively. The overall algorithm is demonstrated at the end of this section. Simulations results are presented in Section IV to verify the effectiveness of proposed algorithms compared with other benchmark schemes. Finally, we conclude the paper in Section V.

II. SYSTEM MODEL AND PROBLEM FORMULATION

A. SYSTEM MODEL

As shown in Fig.1, we consider a UAV-enabled wireless relay system where some confidential information needs to be transmitted from the source S to the destination D via a relay UAV R in the presence of an eavesdropper E. We assume that S, D, E are on the ground with fixed locations, which are known *a priori*. The direct links between ground terminals are assumed negligible due to severe blockage. The UAV mobile relay R is employed to enable communication

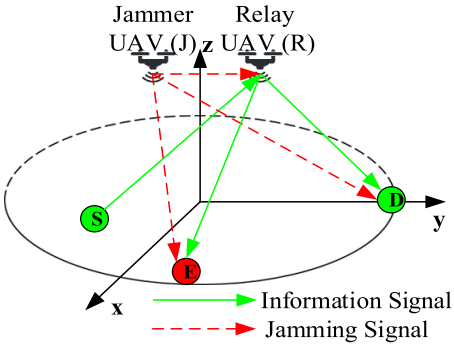

FIGURE 1. An illustration of cooperative UAV-enabled secure mobile relay system.

from S to D. To improve security performance in the system, we introduce a cooperative UAV J as a mobile jammer. The jammer UAV transmits jamming signals to combat against E. Although there is only one eavesdropper on the ground, the system model can be regarded as a standard and integral wiretap system as used in [14]–[16], [19], and [20]. The paper attempts to investigate the effectiveness of the cooperative UAV jamming scheme to improve security performance in a mobile relay system, and we therefore choose a basic system model to study the novel scheme. The proposed scheme and algorithm in the manuscript can be further extended to the scenario where multiple eavesdroppers exist.

Without loss of generality, we consider a three-dimensional (3D) Cartesian coordinate system. The ground user j's horizontal coordinate is denoted by $\mathbf{w}_j = \left[x_j, y_j\right]^T$ in meter (m), $j \in \{\mathrm{S}, \mathrm{D}, \mathrm{E}\}$. Both UAVs are set to fly horizontally at a constant altitude H in m with the pre-determined initial location $\mathbf{q}_0$ and the final location $\mathbf{q}_F$. In practice, the fixed H could correspond to the minimum altitude that is required for obstacle avoidance, and it also helps reduce energy consumption in aircraft ascending or descending. The results in this article can be extended to the case with varying altitudes as well. To simplify the optimization problem, the UAV's flight period T is discretized into N equal-length time slots, i.e., $T = N\delta_t$, where δ_t denotes the elemental slot length. The UAV's trajectory over T can be constructed by using line-segment to connect the optimized N discrete locations $\mathbf{q}_i[n] = [x_i[n], y_i[n]]^T$, where $i \in \{\mathrm{R}, \mathrm{J}\}$, $n \in \mathcal{N} = \{1, \ldots, N\}$. The locations of each UAV in adjacent time slots satisfy the following mobility constraints:

$$\|\mathbf{q}_i[n+1] - \mathbf{q}_i[n]\|^2 \le L^2, \quad n = 1, \ldots, N-1, \tag{1a}$$

$$\|\mathbf{q}_i[1] - \mathbf{q}_{i0}\|^2 \le L^2, \quad \mathbf{q}_i[N] = \mathbf{q}_{iF}, \tag{1b}$$

where L is the maximum horizontal distance that UAV R and J can fly within one time slot under its maximum flight speed V in m/s. For simplicity, we assume that the relay UAV R is equipped with a data buffer of sufficiently large size, and it operates in an FDD mode with equal bandwidth allocated for information reception from S and transmission to D.

The ground-to-ground links between ground terminals, i.e., S-to-D link and S-to-E link are negligible due to

severe blockage. Thus the UAV-enabled secure relay system contains UAV-ground and UAV-to-UAV communication channels. The Doppler effect caused by UAVs' mobility is assumed to be perfectly compensated. The free-space path loss model is adopted in the channel between two UAVs with the power gain at time slot n shown as below

$$h_{ii^*}[n] = \rho_0 d_{ii^*}^{-2}[n] = \frac{\rho_0}{\|\mathbf{q}_i[n] - \mathbf{q}_{i^*}[n]\|^2 + H^2}, \quad n \in \mathcal{N}$$

where ρ_0 denotes the channel power at reference distance $d_0 = 1$ m, d_{ii^*} denotes the distance from UAV i to another UAV i^*, i.e., UAV R to UAV J.

In general, the communication channel between the unmanned aerial vehicle (UAV) and ground users (Gus), denoted by UAV-to-ground communication channel in the paper, includes both line-of-sight (LoS) and non-line-of-sight (NLoS) paths. It is still challenging to find a generally applicable channel model taking such effects into account [23]. Some literature uses the probabilistic LoS model [6], [8]. For the outdoor environment with few high obstructions, there is a high probability of LoS link when the UAV operates at a sufficiently high altitude. Besides, to account for fading effect, the Rician fading model is also commonly adopted [24], which is characterized by a Rician factor to represent the power ratio between the LoS signal component and the scattered signal component. For the multi-path fading environment with a large Rician factor, the LoS channel model gives a reasonable approximation [25]. Therefore, to draw essential insights and for ease of exposition in this paper, we assume that both uplink and downlink UAV-to-ground communications are dominated by LoS links. For the LoS-dominated UAV-to-ground communication links, we adopt the free-space path loss model as used in [3]–[5], [12], and [14]–[17]. It is worth mentioning that the free-space path loss model is one of the considered models in the recent 3GPP specification [26]. In the paper, the path-loss model assumes the path-loss exponent equal to 2, which is a typical large-scale path-loss exponent for the free-space propagation environment. The power gain of the UAV-to-ground channel at time slot n can be written as

$$h_{ij}[n] = \rho_0 d_{ij}^{-2}[n] = \frac{\rho_0}{\|\mathbf{q}_i[n] - \mathbf{w}_j\|^2 + H^2}, \quad n \in \mathcal{N}$$

where ρ_0 denotes the channel power at reference distance $d_0 = 1$ m, d_{ij} denotes the distance from UAV i to a ground terminal j. d_0 is the close-in reference distance, which should be at the far-field of the antenna and determined from measurement close to the transmitter. There are three transmitters in the proposed scheme: the information source, the UAV relay, and the UAV jammer. The transmitters in the information link have limited transmit power. The coverage region of the UAV relay is also limited in our proposed mobile relay system. The communication scenarios considered in this paper can be compared with microcells, where the coverage radius is approximately 100m to 1000m. The UAV-enabled system usually uses the carrier frequency given in the 802.11, LTE, or 5G standard, where 1m is a typical reference distance. In addition, compared with the system in the paper, a lot of references in the paper investigating the UAV-enabled communication models with similar system scale [3]–[5], [12], and [14]–[17]. To make the comparison of simulation results in our proposed scheme with the benchmark schemes more convincing, we consider adopting the generally used reference distance $d_0 = 1$m.

The communication links in the UAV-enabled secure relay system are classified and handled as follows: 1)Legitimate information links: S-to-R and R-to-D. These two links form a dual-hop mobile relay communication link; 2)Eavesdrop link: R-to-E. The ground eavesdropper E wiretaps the UAV relay R; 3)Jammer links: J-to-E, J-to-R, and J-to-D. The signal transmitted by the UAV jammer J is regarded as noise for other terminals, i.e., R, D, and E.

Let $\mathbf{P}_R$ and $\mathbf{P}_J$ denote the transmit power of the relay UAV R and the jammer UAV J, respectively. In time slot n, UAV R forwards the information signal, while UAV J transmits the jamming signal. $\mathbf{P}_R$ and $\mathbf{P}_J$ are subject to both average and peak power constraints as follows

$$\sum_{n=1}^{N} P_R[n] \le N\bar{P}_R, \quad 0 \le P_R[n] \le P_{R\max}, \ n \in \mathcal{N}, \tag{2a}$$

$$\sum_{n=1}^{N} P_J[n] \le N\bar{P}_J, \quad 0 \le P_J[n] \le P_{J\max}, \ n \in \mathcal{N}, \tag{2b}$$

where $\bar{P}_R \le P_{R_{\max}}$ and $\bar{P}_J \le P_{J_{\max}}$. In the proposed scheme, the average power constraint on the UAV is meaningful. The maximum power constraint is a direct power constraint for each time slot in the optimization problem, which is related to the limitation of the real-time transmit power of the device. However, the average power constraint is actually a limitation on the total power over the entire process of the optimization problem, which is also corresponding to the energy-efficient consideration in the system [5], [14], [16], [19], [20], [23], [27]. In our paper, we propose a cooperative security scheme to improve the secrecy rate in the UAV-enabled mobile relay system and schemes in [14], [19], and [20] are also the benchmarks in the simulations. We assume that the transmit power of source S is a constant denoted by P_S greater than $P_{R_{\max}}$ and $P_{J_{\max}}$.

The maximum transmission rate from S to R in bit/second/Hz (bps/Hz) for slot n can be expressed as

$$R_R[n] = \log_2\left(1 + \frac{P_S \hat{h}_{SR}[n]}{P_J[n]\hat{h}_{JR}[n] + 1}\right), \tag{3}$$

where $\hat{h}_{ii^*}[n] = \frac{\gamma_0}{\|\mathbf{q}_i[n] - \mathbf{q}_{i^*}[n]\|^2 + H^2}, i, i^* \in \{J, R\}, i \ne i^*, n \in \mathcal{N}$; $\hat{h}_{ij}[n] = \frac{\gamma_0}{\|\mathbf{q}_i[n] - \mathbf{w}_j\|^2 + H^2}, i \in \{J, R\}, j \in \{S, D, E\}, n \in \mathcal{N}$; σ^2 denotes the noise power and $\gamma_0 = \frac{\rho_0}{\sigma^2}$.

Similarly, the achievable rate from R to D at slot n can be expressed as

$$R_D[n] = \log_2\left(1 + \frac{P_R[n]\hat{h}_{RD}[n]}{P_J[n]\hat{h}_{JD}[n] + 1}\right), \tag{4}$$

and the achievable rate of wiretapping channel R-to E in bps/Hz at time slot n can be written as

$$R_E[n] = \log_2\left(1 + \frac{P_R[n]\hat{h}_{RE}[n]}{P_J[n]\hat{h}_{JE}[n] + 1}\right). \tag{5}$$

In practical situations, at each slot n, the relay UAV R can only forward the data that has already been received from S. Thus, the *information-causality constraint* introduced in section I is imposed on the relay UAV R by assuming that the processing delay at R is one slot [5].

$$\sum_{i=2}^{n} R_D[i] \le \sum_{i=1}^{n-1} R_R[i], \quad n = 2, \ldots, N. \tag{6}$$

We adopt average achievable secrecy rate as the measurement of system security performance. With (4) and (5), the average achievable secrecy rate of the cooperative UAV-enabled relay system in bps/Hz over N time slots is given by

$$R_{sec} = \frac{1}{N}\sum_{n=1}^{N-1}[R_D[n] - R_E[n]]^+, \tag{7}$$

where $[x]^+ \triangleq \max(x, 0)$.

B. PROBLEM FORMULATION

Taking the *information-causality constraint* (6) into account, we aim to maximize the average achievable secrecy rate (7) by jointly optimizing trajectory and transmit power for both the relay UAV and the jammer UAV over all time slots. The optimization problem is formulated as

$$\begin{aligned}(\text{P1}): \max_{\mathbf{Q}_J, \mathbf{Q}_R, \mathbf{P}_S, \mathbf{P}_U} & \sum_{n=1}^{N-1}(R_D[n] - R_E[n]) \\ \text{s.t. } & (1a), (1b), (2a), (2b), (6),\end{aligned}$$

where the operation $[\cdot]^+$ is omitted. Since we can guarantee non-negativity on each term in the summation through setting $P_R[n] = 0$.

(P1) is a non-convex optimization problem and therefore can not be directly solved with standard convex optimization techniques. To solve (P1), we need to tackle the following difficulties: 1) In objective function and constraints of (P1), both the numerator and the denominator of the fractions in R_D, R_E, and R_R have trajectory and transmit power optimization variables; 2) the non-convex *information-causality constraint* is tough to handle, which makes our problem (P1) more difficult to tackle; 3) the objective function is not concave though the $[\cdot]^+$ operation is removed.

III. PROPOSED SOLUTION FOR (P1)

In this section, we apply update-rate-assisted block coordinate descent and successive convex approximation techniques to propose an effective algorithm sloving problem (P1). Problem (P1) is decoupled into four subproblems to optimize relay UAV's trajectory $\mathbf{Q}_R$, jammer UAV's trajectory $\mathbf{Q}_J$, relay UAV's transmit power $\mathbf{P}_R$ and jammer UAV's transmit power $\mathbf{P}_J$. By introducing an update rate λ, the optimization variables can be optimized alternately in an iterative manner until the algorithm converges.

According to the system model and proposed scheme, we choose to divide the problem into four subproblems, which is necessary for the following reasons. First, the resources on UAVs are distinguished. It is common to split the transmit power and flight trajectory of a UAV into two groups of variables and optimize them respectively, [5], [16], [23], [27]. The problem of simultaneously optimizing the power and the trajectory usually has fractions with both the numerator and the denominator containing the trajectory and transmit power optimization variables, which is usually non-convex and even not a fractional programming problem. We therefore consider optimizing the transmit power and trajectory respectively instead of simultaneously optimizing all the resources on a UAV. Second, the roles of UAVs are distinguished. There is also a method to divide the original problem into two subproblems. That is optimizing the power and trajectory of all UAVs, respectively. In this method, we can regard the power optimization of all UAVs as a subproblem while the trajectory optimization of all UAVs as another subproblem. Though the UAVs' trajectories can be optimized simultaneously [27], the UAVs are set with similar functions in the flight mission. In [27], all the UAVs are deployed as aerial base stations. However, in our proposed scheme, the UAVs have different roles: the jammer and the relay. It is unreasonable to optimize the same resource on all UAVs containing different roles at the same time. Thus, the author splits the problem into four subproblems to distinguish the roles of UAVs and the resources on UAV [15], [18]. This partition can also be further applied to the multi-jammer or multi-relay scenarios, where the four subproblems are the trajectory optimization for all jammer UAVs, the power optimization for all jammer UAVs, the trajectory optimization for all relay UAVs, and the power optimization for all relay UAVs.

A. OPTIMIZING RELAY UAV's TRANSMIT POWER $\mathbf{P}_R$

For any given relay UAV's trajectory $\mathbf{Q}_R$, jammer UAV's trajectory $\mathbf{Q}_J$, and jammer UAV's transmit power $\mathbf{P}_J$, the original problem (P1) can be recast as

$$(\text{P2}): \max_{\mathbf{P}_R} \sum_{n=1}^{N}\left[\log_2(1 + a_n P_R[n]) - \log_2(1 + b_n P_r[n])\right] \tag{8a}$$

$$\text{s.t.} \sum_{i=2}^{n}\log_2(1 + a_i P_R[i]) \le \sum_{i=1}^{n-1} R_R[i], \quad n = 2, \ldots, N, \quad (2a), \tag{8b}$$

where $a_n = \frac{\hat{h}_{RD}[n]}{P_J[n]\hat{h}_{JD}[n]+1}$, $b_n = \frac{\hat{h}_{RE}[n]}{P_J[n]\hat{h}_{JE}[n]+1}$.

If (8b) is removed, subproblem (P2) has a closed-form solution [28]. However, the additional *information-causality constraint* makes (P2) a non-convex problem. To handle

the non-convexity of (8b) and (8a) with respect to $\mathbf{P}_R$, the successive convex approximation technique is applied. $-\log_2(1+b_nP_r[n])$ and $\log_2(1+a_iP_r[i])$ can be replaced by their respective convex lower bound and concave upper bound at a given local point. Denote $\mathbf{P}_r^k = \left\{P_r^k[n], n\in\mathcal{N}\right\}$ as the result of relay UAV's transmit power after kth iteration. By using the property that the first-order Taylor approximation of a convex function is a global under-estimate [29], we have following inequalities:

$$-\log_2(1+b_nP_R[n]) \geq A^k[n]\left(P_R[n]-P_R^k[n]\right)+B^k[n] \tag{9a}$$

$$\log_2(1+a_iP_R[i]) \leq C^k[i]\left(P_R[i]-P_R^k[i]\right)+F^k[i] \tag{9b}$$

where $A^k[n] = \frac{-b_n}{\ln 2\left(1+b_nP_R^k[n]\right)}$, $C^k[i] = \frac{a_i}{\ln 2\left(1+a_iP_R^k[i]\right)}$, $B^k[n] = -\log_2\left(1+b_nP_R^k[n]\right)$, $F^k[i] = \log_2\left(1+b_iP_R^k[i]\right)$

With (9), the problem (P2) can be reformulated as

$$\text{(P2')}: \max_{\mathbf{P}_R}\sum_{n=1}^{N}\left\{\log_2(1+a_nP_R[n])+A^k[n]P_R[n]\right\} \tag{10a}$$

$$\text{s.t.}\sum_{i=2}^{n}\left(C^k[i]\left(P_R[i]-P_R^k[i]\right)+F^k[i]\right) \leq \sum_{i=1}^{n-1}R_R[i], \quad n=2,\ldots,N. \quad (2a). \tag{10b}$$

For any existing relay UAV's transmit power $\left\{P_R^k[n]\right\}$, the left-hand side (LHS) of constraint (8b) is upper bound by the LHS of (10b), and (P2') maximizes the lower bound of the objective function of its original problem (P2). Thus, the objective value of (P2) is lower bounded by that of the problem (P2'). Moreover, since the first-order Taylor expansions in (9) suggest that the objective value of (P2) at $\mathbf{P}_R^k$ is the same as that of (P2'), which means that the objective value of (P2) with the solution obtained by solving (P2') is always no less than that with any $\mathbf{P}_R^k$ in each iteration. Note that (P2') is a convex optimization problem and can be efficiently solved by existing convex optimization tools such as CVX [30].

B. OPTIMIZING JAMMER UAV's POWER $\mathbf{P}_J$

Knowing the jammer UAV's trajectory $\mathbf{Q}_J$, the relay UAV's trajectory $\mathbf{Q}_R$ and transmit power $\mathbf{P}_R$, problem (P1) can be recast as

$$\text{(P3)}: \max_{\mathbf{P}_J}\sum_{n=1}^{N}\left[\log_2\left(1+\frac{c_n}{g_nP_J[n]+1}\right)-\log_2\left(1+\frac{e_n}{f_nP_J[n]+1}\right)\right] \tag{11a}$$

$$\text{s.t.}\sum_{i=2}^{n}\log_2\left(1+\frac{c_i}{g_iP_J[i]+1}\right) \leq \sum_{i=1}^{n-1}\log_2\left(1+\frac{l_i}{m_iP_J[i]+1}\right), \quad n=2,\ldots,N, \quad (3b), \tag{11b}$$

where $c_n = P_R[n]\hat{h}_{RD}[n]$, $g_n = \hat{h}_{JD}[n]$, $e_n = P_R[n]\hat{h}_{RE}[n]$, $f_n = \hat{h}_{JE}[n]$, $l_i = P_S\hat{h}_{SR}[i]$, $m_i = \hat{h}_{JR}[i]$ are constants in subproblem (P3).

Similar to (P2), we apply successive convex approximation technique to deal with the non-convex objective function (11a) and the *information-causality constraint* (11b). $\log_2\left(1+\frac{c_n}{g_nP_J[n]+1}\right)$ and $\log_2\left(1+\frac{l_i}{m_iP_J[i]+1}\right)$ are convex function as $c_n, g_n, l_i, m_i \geq 0$, thus we can use the first-order Taylor approximation to find their lower bound and obtain following inequalities

$$\log_2\left(1+\frac{c_n}{g_nP_J[n]+1}\right) \geq G^k[n]\left(P_J[n]-P_J^k[n]\right)+I^k[n] \tag{12a}$$

$$\log_2\left(1+\frac{l_i}{m_iP_J[i]+1}\right) \geq L^k[n]\left(P_J[i]-P_J^k[i]\right)+M^k[i] \tag{12b}$$

where $G^k[n] = \frac{-c_ng_n}{\ln 2\left(g_nP_J^k[n]+1\right)\left(g_nP_J^k[n]+c_n+1\right)}$, $I^k[n] = \log_2\left(1+\frac{c_n}{g_nP_J^k[n]+1}\right)$, $M^k[i] = \log_2\left(1+\frac{l_i}{g_iP_J^k[i]+1}\right)$, $L^k[n] = \frac{-l_im_i}{\ln 2\left(m_iP_J^k[i]+1\right)\left(m_iP_J^k[i]+l_i+1\right)}$.

With (12), the problem (P3) can be reformulated as

$$\text{(P3')}: \max_{\mathbf{P}_J}\sum_{n=1}^{N}\left\{G^k[n]P_J[n]-\log_2\left(1+\frac{e_n}{f_nP_J[n]+1}\right)\right\} \tag{13a}$$

$$\text{s.t.}\sum_{i=2}^{n}\log_2\left(1+\frac{c_i}{g_iP_J[i]+1}\right) \leq L^k[n]\left(P_J[i]-P_J^k[i]\right)+M^k[i], \quad n=2,\ldots,N, \quad (3b). \tag{13b}$$

(P3') has a concave objective function and convex constraints. Thus, (P3') is a convex optimization problem and can be efficiently solved by CVX. Similar with section III-A, it can be shown that the objective value of (P3) with the solution obtained by solving (P3') is always no less than that with any $\mathbf{P}_J^k$ and the optimal value of transformed problem (P3') serves as lower bound for that of original problem (P3).

C. OPTIMIZING JAMMER UAV's TRAJECTORY $\mathbf{Q}_J$

The trajectory optimization problems with fixed transmit power in our model have a more complex objective function and optimization constraints compared with the previous

power optimization problems. For any given relay UAV's trajectory $\mathbf{Q}_R$ and both UAVs' transmit power $\mathbf{P}_Q, \mathbf{P}_J$, we can derive following jammer UAV's trajectory $\mathbf{Q}_J$ optimization subproblem (P4):

$$(\text{P4}): \max_{\mathbf{Q}_J} \sum_{n=1}^{N} \left[\log_2 \left(1 + \frac{c_n}{\frac{\lambda_0 P_J[n]}{\|\mathbf{q}_J[n]-\mathbf{w}_D\|^2+H^2}+1} \right) - \log_2 \left(1 + \frac{e_n}{\frac{\lambda_0 P_J[n]}{\|\mathbf{q}_J[n]-\mathbf{w}_E\|^2+H^2}+1} \right) \right] \tag{14a}$$

$$\text{s.t} \sum_{i=2}^{n} \log_2 \left(1 + \frac{c_i}{\frac{\lambda_0 P_J[i]}{\|\mathbf{q}_J[i]-\mathbf{w}_D\|^2+H^2}+1} \right) \leq \sum_{i=1}^{n-1} \log_2 \left(1 + \frac{l_i}{\frac{\lambda_0 P_J[i]}{\|\mathbf{q}_J[i]-\mathbf{q}_R[i]\|^2+H^2}+1} \right), \quad n = 2, \ldots, N, \quad (1), i = J. \tag{14b}$$

By introducing slack variables $\mathbf{S}, \mathbf{V}, \mathbf{U}, \mathbf{R}_D^{slack}$ as follows: $\mathbf{S} = \left\{ s[n] = \|\mathbf{q}_J[n] - \mathbf{w}_D\|^2 + H^2, n \in \mathcal{N} \right\}$, $\mathbf{V} = \left\{ v[n] = \|\mathbf{q}_J[n] - \mathbf{q}_R[n]\|^2 + H^2, n \in \mathcal{N} \right\}$, $\mathbf{U} = \left\{ u[n] = \|\mathbf{q}_J[n] - \mathbf{w}_E\|^2 + H^2, n \in \mathcal{N} \right\}$, $\mathbf{R}_D^{slack,J} = \left\{ R_D^{slack,J}[n], n \in \mathcal{N} \right\}$, problem (P4) can be expressed as

$$(\text{P4.1}): \max_{\mathbf{Q}_J, \mathbf{S}, \mathbf{V}, \mathbf{U}, \mathbf{R}_D^{slack,J}} \sum_{n=1}^{N} \left\{ R_D^{slack,J}[n] - \log_2 \left(1 + \frac{e_n}{\frac{\lambda_0 P_J[n]}{u[n]}+1} \right) \right\} \tag{15a}$$

$$\text{s.t. } s[n] - \|\mathbf{q}_J[n] - \mathbf{w}_D\|^2 - H^2 \leq 0, \quad \forall n, \tag{15b}$$

$$\|\mathbf{q}_J[n] - \mathbf{w}_E\|^2 + H^2 - u[n] \leq 0, \quad \forall n, \tag{15c}$$

$$v[n] - \|\mathbf{q}_J[n] - \mathbf{q}_R[n]\|^2 - H^2 \leq 0, \quad \forall n, \tag{15d}$$

$$\sum_{i=2}^{n} R_D^{slack,J}[i] - \sum_{i=1}^{n} \log_2 \left(1 + \frac{l_i}{\frac{\lambda_0 PJ[i]}{v[i]}+1} \right) \leq 0, \quad n = 2, \ldots, N, \tag{15e}$$

$$R_D^{slack,J}[n] \leq \log_2 \left(1 + \frac{c_n}{\frac{\lambda_0 P_J[n]}{s[n]}+1} \right), \quad n = 2, \ldots, N, \quad (1), i = J. \tag{15f}$$

It can be verified that at the optimal solution to problem (P4), constraints (15b), (15c), and (15d) must hold with equalities, since otherwise $u[n]$ can be decreased to improve the objective value and $s[n]$, $v[n]$ can be increased to relax constraint (15e) and (15f) which means (P4.1) can be further optimized. Thus, the optimal value of (P4) is lower-bounded by that of (P4.1) owing to slack variables $\mathbf{R}_D^{slack,J}$. However, (P4.1) is still a non-convex optimization problem due to non-convexity on the second term in summation function $\log_2 \left(1 + \frac{e_n}{\frac{\lambda_0 P_J[n]}{u[n]}+1} \right)$ and left-hand side of constraints (15b) and (15d). Define $\mathbf{Q}_J^k = \left\{ \mathbf{q}_J^k[n], n \in \mathcal{N} \right\}$ as a given initial trajectory of relay UAV J in the $k+1$-th iteration. Successive convex approximation technique is applied where terms $\log_2 \left(1 + \frac{e_n}{\frac{\lambda_0 P_J[n]}{u[n]}+1} \right)$, $-\|\mathbf{q}_J[n] - \mathbf{w}_D\|^2$, and $-\|\mathbf{q}_J[n] - \mathbf{q}_R[n]\|^2$ are replaced by their respective concave upper bound at a given local point as follows

$$\log_2 \left(1 + \frac{e_n}{\frac{\gamma_0 P_J[n]}{u[n]}+1} \right) \leq W^k[n] \left(u[n] - u^k[n] \right) + X^k[n], \tag{16a}$$

$$-\|\mathbf{q}_J[n] - w_D\|^2 \leq Y^k[n], \tag{16b}$$

$$-\|\mathbf{q}_J[n] - \mathbf{q}_R[n]\|^2 \leq Z^k[n], \tag{16c}$$

where $W^k[n] = \frac{e_n \gamma_0 P_J[n]}{\ln 2 (u^k[n]+\gamma_0 P_J[n])((e_n+1)u^k[n]+\gamma_0 P_J[n])}$, $X^k[n] = \log_2 \left(1 + \frac{e_n u^k[n]}{\gamma_0 P_J[n]+u^k[n]} \right)$, $u^k[n] = \|\mathbf{q}_J - \mathbf{w}_E\| + H^2$, $Y^k[n] = \|\mathbf{q}_J^k[n]\|^2 - 2\left[\mathbf{q}_J^k[n] - \mathbf{w}_D\right]^T \mathbf{q}_J[n] - \|\mathbf{w}_D\|^2$, $Z^k[n] = \|\mathbf{q}_J^k[n]\|^2 - 2\left[\mathbf{q}_J^k[n] - \mathbf{q}_R[n]\right]^T \mathbf{q}_J[n] - \|\mathbf{q}_R[n]\|^2$.

With (16), problem (P4.1) can be recast as

$$(\text{P4.2}): \max_{\mathbf{Q}_J, \mathbf{S}, \mathbf{V}, \mathbf{U}, \mathbf{R}_D^{slack,J}} \sum_{n=1}^{N} \left(R_D^{slack,J}[n] - W^k[n] u[n] \right) \tag{17a}$$

$$\text{s.t. } s[n] + Y_k[n] - H^2 \leq 0, \quad \forall n, \tag{17b}$$

$$v[n] + Z^k[n] - H^2 \leq 0, \quad \forall n, \tag{17c}$$

$$(15c), (15e), (15f), (1), \quad i = J.$$

Note that (P4.2) is a convex optimization problem which can be efficiently solved by the interior-point method. As a result, the slack problem (P4.1) is approximately solved based on the optimal solution to (P4.2). The optimal value of (P4.2) serves as a lower bound for that of (P4.1). Meanwhile, the optimal value of (P4) is lower-bounded by that of (P4.1). It can be shown that the resulting optimal values of (P4.2) are no less than that with any $\mathbf{Q}_J^k$ and further upper-bounded by the optimal value of (P4). Thus, the original problem (P4) can be approximately solved by solving (P4.2) iteratively. The current optimal solution gradually approaches the optimal solution to (P4) as the number of iterations increases. Furthermore, the iteration will eventually converge to the point that satisfies the Karush-Kuhn-Tucker (KKT) optimality conditions of the original problem (P4) [17].

D. OPTIMIZING RELAY UAV's TRAJECTORY $\mathbf{Q}_R$

For any given jammer UAV's trajectory $\mathbf{Q}_J$ and both UAVs' transmit power $\mathbf{P}_R, \mathbf{P}_J$, we can derive following optimization

subproblem on the relay UAV's trajectory (P5):

$$\begin{aligned}(\text{P5}):\ \max_{\mathbf{Q}_R}\ &\sum_{n=1}^{N}\left[\log_2\left(1+\alpha_n\frac{1}{\|\mathbf{q}_R[n]-\mathbf{w}_D\|^2+H^2}\right)\right.\\&\left.-\log 2\left(1+\mu_n\frac{1}{\|\mathbf{q}_R[n]-\mathbf{w}_E\|^2+H^2}\right)\right] \qquad (18a)\\ \text{s.t.}\ &\sum_{i=2}^{n}\log_2\left(1+\alpha_i\frac{1}{\|\mathbf{q}_R[i]-\mathbf{w}_D\|^2+H^2}\right)\\&\le\sum_{i=1}^{n-1}\log_2\left(1+\frac{P_S\frac{\lambda_0}{\|\mathbf{q}_R[n]-\mathbf{w}_S\|^2+H^2}}{P_J[n]\frac{\lambda_0}{\|\mathbf{q}_R[n]-\mathbf{q}_R[n]\|^2+H^2}}\right)\\&n=2,\ldots,N,\quad (1),i=J, \qquad (18b)\end{aligned}$$

where $\alpha_n=\frac{P_R[n]\lambda_0}{P_J[n]\hat{h}_{JD}[n]+1}$, $\mu_n=\frac{P_R[n]\lambda_0}{P_J[n]\hat{h}_{JE}[n]+1}$ are constant in this subproblem.

The optimization problem (P5) has a non-concave objective function in (18a) and a non-convex constraint in (18b), thus (P5) is difficult to solve directly. Moreover, trajectory optimization variables $\mathbf{Q}_R$ exist in both the numerator and the denominator of the fractions in the right-hand side of (18b), which makes our problem (P5) tough to tackle.

To facilitate solving subproblem (P5), we introduce slack variables $\{t[n]\}$, $\{x[n]\}$, $\{y[n]\}$ and $\left\{R_D^{slack,R}[n]\right\}$. With these slack variables, we can transform the problem into a more tractable form:

$$\begin{aligned}(\text{P5.1}):\ \max_{\mathbf{Q}_R,\mathbf{T},\mathbf{X},\mathbf{Y},\mathbf{R}_D^{slack,R}}\ &\sum_{n=1}^{N}\left\{R_D^{slack,R}[n]\right.\\&\left.-\log_2\left(1+\mu_n\frac{1}{H^2+t[n]}\right)\right\} \qquad (19a)\\ \text{s.t.}\ &t[n]\le\|\mathbf{q}_R[n]-\mathbf{w}_E\|^2,\quad \forall n, \qquad (19b)\\&\sum_{i=2}^{n}R_D^{slack,R}[i]\le\sum_{i=1}^{n-1}\frac{1}{\ln 2}(x[n]-y[n]),\\&n=2,\ldots,N, \qquad (19c)\\&P_S\hat{h}_{SR}[n]+P_J[n]\hat{h}_{JR}[n]+1\ge e^{x[n]},\\&\forall n, \qquad (19d)\\&P_J[n]\hat{h}_{JR}[n]+1\le e^{y[n]},\quad \forall n, \qquad (19e)\\&R_D^{slack,R}\\&\le\log_2\left(1+\alpha_n\frac{1}{\|\mathbf{q}_R[i]-\mathbf{w}_D\|^2+H^2}\right)\\&n=2,\ldots,N,\quad (1),i=J, \qquad (19f)\end{aligned}$$

where $\mathbf{X}=\{x[n],n\in\mathcal{N}\}$, $\mathbf{Y}=\{y[n],n\in\mathcal{N}\}$, $\mathbf{T}=\{t[n],n\in\mathcal{N}\}$, $\mathbf{R}_D^{slack,R}=\left\{R_D^{slack,R}[n],n\in\mathcal{N}\right\}$.

The transformed problem (P5.1) is still a non-convex problem due to non-convexity constraints (19b), (19d), (19e), and (19f). Similar as the analysis in section II part C, (19b), (19d), and (19e) must hold with equalities at the optimal solution and (P5.1) serves as lower bound to the original problem (P5) owing to slack variables $\mathbf{R}_D^{slack,R}$.

Then we focus on tackling the non-convex constraints in (P5.1). In the following formulas, $\mathbf{q}_R^k[n]$ is a given initial location of relay UAV J in the $k+1$-th iteration on time slot n defined by $\mathbf{Q}_R^k=\left\{\mathbf{q}_R^k[n],n\in\mathcal{N}\right\}$.

First, successive convex approximation technique is applied on (19b). We can derive the following inequalities by utilizing the first-order Taylor expansion of $\|\mathbf{q}_R[n]-\mathbf{w}_E\|^2$ with respect to $\mathbf{q}_R[i]$:

$$\begin{aligned}&\|\mathbf{q}_R[n]-\mathbf{w}_E\|^2\ge\Gamma^k[n]\\&\triangleq\|\mathbf{q}_R^k[n]-\mathbf{w}_E\|^2\\&\quad+2\left(\mathbf{q}_R^k[n]-\mathbf{w}_E\right)^T\left(\mathbf{q}_R[n]-\mathbf{q}_R^k[n]\right). \qquad (20)\end{aligned}$$

With (20), (19b) can be substituted by the convex constraint (21). The left-hand side of (21) is an affine function.:

$$t[n]-\Gamma^k[n]\le 0 \qquad (21)$$

Second, it can be shown that $\hat{h}_{SR}[n]$, $\hat{h}_{JR}[n]$ and $\log_2\left(1+\alpha_n\frac{1}{\|\mathbf{q}_R[i]-\mathbf{w}_D\|^2+H^2}\right)$ are convex function of their corresponding norm term $\|\mathbf{q}_R[n]-\mathbf{q}_J[n]\|^2$ and $\|\mathbf{q}_R[n]-\mathbf{w}_D\|^2$. Thus the first-order Taylor expansion can be applied on (19f) and (19d) with respect to their norm term $\|\mathbf{q}_R[n]-\mathbf{q}_J[n]\|^2$ and $\|\mathbf{q}_R[n]-\mathbf{w}_D\|^2$ to obtain the convex lower bound.

$$\begin{aligned}\hat{h}_{SR}[n]=&\frac{\lambda_0}{\|\mathbf{q}_R[n]-\mathbf{w}_S\|^2+H^2}\ge\hat{h}_{SR}^{lb}[n]\\\triangleq&\frac{2\lambda_0}{\|\mathbf{q}_R^k[n]-\mathbf{w}_S\|^2+H^2}\\&-\frac{\lambda_0\left(\|\mathbf{q}_R[n]-\mathbf{w}_S\|^2+H^2\right)}{\left(\|\mathbf{q}_R^k[n]-\mathbf{w}_S\|^2+H^2\right)^2} \qquad (22a)\\\hat{h}_{JR}[n]=&\frac{\lambda_0}{\|\mathbf{q}_R[n]-\mathbf{q}_J[n]\|^2+H^2}\ge\hat{h}_{JR}^{lb}[n]\\\triangleq&\frac{2\lambda_0}{\|\mathbf{q}_R^k[n]-\mathbf{q}_J[n]\|^2+H^2}\\&-\frac{\lambda_0\left(\|\mathbf{q}_R[n]-\mathbf{q}_J[n]\|^2+H^2\right)}{\left(\|\mathbf{q}_R^k[n]-\mathbf{q}_J[n]\|^2+H^2\right)^2} \qquad (22b)\\\log_2\left(1+\alpha_n\frac{1}{\|\mathbf{q}_R[n]-\mathbf{w}_D\|^2+H^2}\right)\ge&\hat{R}_D^{lb}[n]\\\triangleq&\log_2\left(1+\alpha_n\frac{1}{\|\mathbf{q}_R^k[n]-\mathbf{w}_D\|^2+H^2}\right)\\&+\left(\frac{-\alpha_n/\ln 2}{1+\alpha_n\frac{1}{\|\mathbf{q}_R^k[n]-\mathbf{w}_D\|^2+H^2}}\right)\\&\times\frac{\|\mathbf{q}_R[n]-\mathbf{w}_D\|^2-\|\mathbf{q}_R^k[n]-\mathbf{w}_D\|^2}{\|\mathbf{q}_R^k[n]-\mathbf{w}_D\|^2+H^2} \qquad (23)\end{aligned}$$

With (23), constraint (19f) can be transformed to

$$R_D^{slack,R}\le\hat{R}_D^{lb}[n] \qquad (24)$$

(24) has only affine functions on both sides, so it is convex. For (19d), combined (22) with constants in the original inequalities, we can derive following inequalities

$$P_S \hat{h}_{SR}^{lb}[n] + P_J[n] \hat{h}_{JR}^{lb}[n] + 1 - e^{x[n]} \geq 0. \tag{25}$$

It can be observed that the left-hand side of (25) is jointly concave with respect to optimization variables $\mathbf{q}_R[n]$ and $x[n]$. After the previous processing, only constraints (19e) are left to handle. We introduce slack variables $\Phi = \left\{\varphi[n] = \|\mathbf{q}_R[n] - \mathbf{q}_J[n]\| + H^2, n \in \mathcal{N}\right\}$ to transform the difference of two convex functions in (19e) into the following inequalities.

$$\frac{\gamma_0 P_J[n]}{\varphi[n]} + 1 \leq e^{y[n]} \tag{26a}$$

$$\|\mathbf{q}_R[n] - \mathbf{q}_J[n]\| + H^2 - \varphi[n] \geq 0 \tag{26b}$$

It can be shown at the optimal value of (P5.1), (26b) must hold with equality. Otherwise $\varphi[n]$ can be increased to relax constraint (26a), which further relax original constraint (19e). However, though (19e) has been transformed, (26a) and (26b) are still non-convex. We apply successive convex approximation technique on them respectively by utilizing the following inequalities:

$$e^{y[n]} \geq e^{y^k[n]}\left(y[n] - y^k[n] + 1\right), \tag{27a}$$

$$\|\mathbf{q}_R[n] - \mathbf{q}_J[n]\| \geq \Delta^k[n] \triangleq \|\mathbf{q}_R^k[n] - \mathbf{q}_J[n]\|^2 + 2\left(\mathbf{q}_R^k[n] - \mathbf{q}_J[n]\right)^T\left(\mathbf{q}_R[n] - \mathbf{q}_R^k[n]\right). \tag{27b}$$

Combined with (27), (19e) can be replaced by convex constraints as follows

$$\frac{\gamma_0 P_J[n]}{\varphi[n]} + 1 \leq e^{y^k[n]}\left(y[n] - y^k[n] + 1\right), \tag{28a}$$

$$\varphi[n] - \Delta^k[n] \leq 0. \tag{28b}$$

According to the above transformation, the non-convex constraints in (P5.1) are replaced by transformed convex constraints and (P5.1) is therefore recast as

$$\begin{aligned}(\text{P5.2}): \max_{\mathbf{Q}_R,\mathbf{T},\mathbf{X},\mathbf{Y},\mathbf{R}_D^{slack,R}} & \sum_{n=1}^{N}\left\{R_D^{slack,R}[n] - \log_2\left(1 + \mu_n \frac{1}{H^2 + t[n]}\right)\right\} \\ \text{s.t. } & (19c), (21), (24), (25), (28), (1), \\ & i = R.\end{aligned} \tag{29}$$

As a result, the optimal objective value of (P5.2) serves as a lower bound for that of the slack problem (P5.1). Then (P5.1) can be approximately solved based on the optimal solution to (P5.2). At the same time, the optimal value of (P5) is lower-bounded by that of (P5.1), while the resulting optimal values of (P5.2) are no less than that with any $\mathbf{Q}_R^k$ and further upper-bounded by the optimal value of (P5). The above analysis illustrates that the convergence of the proposed algorithm to (P5) theoretically, and the original problem (P5) can be approximately solved by solving (P5.2). Note that (P5.2) is a convex optimization problem and can be efficiently solved by the interior-point method. Similar to section III-C, the original problem (P5) can be solved by iteratively optimizing (P5.2) until achieving the convergence.

Algorithm 1 Proposed Iterative Algorithm C-T&P for (P1)

1: Initialize relay UAV's trajectory $\mathbf{Q}_R^0$, jammer UAV's trajectory $\mathbf{Q}_J^0$, relay UAV's transmit power $\mathbf{P}_R^0$, jammer UAV's transmit power $\mathbf{P}_J^0$, update rate η and iteration times $k = 0$.
2: **repeat**
3: Set $k = k + 1$, $\eta = \eta/(1 + (k-1) * \xi)$.
4: Given feasible solution $\left(\mathbf{P}_R^{k-1}, \mathbf{P}_J^{k-1}, \mathbf{Q}_R^{k-1}, \mathbf{Q}_J^{k-1}\right)$, solve problem (P4.2) and obtain corresponding optimal solution $\tilde{\mathbf{Q}}_J^k$, then update the current solution as $\mathbf{Q}_J^k = \eta\left(\tilde{\mathbf{Q}}_J^k - \mathbf{Q}_J^{k-1}\right) + \mathbf{Q}_J^{k-1}$.
5: Given feasible solution $\left(\mathbf{P}_R^{k-1}, \mathbf{P}_J^{k-1}, \mathbf{Q}_R^{k-1}, \mathbf{Q}_J^{k}\right)$, solve problem (P5.2) and obtain corresponding optimal solution $\tilde{\mathbf{Q}}_R^k$, then update the current solution as $\mathbf{Q}_R^k = \eta\left(\tilde{\mathbf{Q}}_R^k - \mathbf{Q}_R^{k-1}\right) + \mathbf{Q}_R^{k-1}$.
6: Given feasible solution $\left(\mathbf{P}_R^{k-1}, \mathbf{P}_J^{k-1}, \mathbf{Q}_R^{k}, \mathbf{Q}_J^{k}\right)$, solve problem (P3') and obtain corresponding optimal solution $\tilde{\mathbf{P}}_J^k$, then update the current solution as $\mathbf{P}_J^k = \eta\left(\tilde{\mathbf{P}}_J^k - \mathbf{P}_J^{k-1}\right) + \mathbf{P}_J^{k-1}$.
7: Given feasible solution $\left(\mathbf{P}_R^{k-1}, \mathbf{P}_J^{k}, \mathbf{Q}_R^{k}, \mathbf{Q}_J^{k}\right)$, solve problem (P2') and obtain corresponding optimal solution $\tilde{\mathbf{P}}_R^k$, then update the current solution as $\mathbf{P}_R^k = \eta\left(\tilde{\mathbf{P}}_R^k - \mathbf{P}_R^{k-1}\right) + \mathbf{P}_R^{k-1}$.
8: Calculate and update objective value in (P1) with current optimal solution.
9: **until** the increase of the objective value in (P1) is less than a threshold ε.

E. OVERALL ALGORITHM

In the previous section III-A, B, C, and D, we have obtained solutions for four subproblems, respectively. Based on the solutions to the subproblems, we apply block coordinate descent method to solve (P2'), (P3'), (P4.2), and (P5.2) alternately in an iterative manner and the original problem (P1) is thus solved approximately. The proposed algorithm terminates when the fractional increase of the objective value is below a given threshold $\varepsilon > 0$. The convergence of Algorithm 1 is proved by reference to [3] shown in (30)-(34) this section. The proposed algorithm generally converges to a locally optimal solution. In our proposed scheme, the algorithm applying the update-rate-assisted block coordinate descent and successive convex approximation techniques is a heuristic algorithm. Thus, the global optimality cannot be guaranteed [5]. Decoupling the original problem

weakens the relevance of variables in different subproblems. Thus, we introduce update-rate inspired by learning-based algorithms. The update rate in our proposed algorithm is denoted by $\eta \in [0, 1]$. In k-th iteration, the η is updated by $\eta = \eta/(1 + (k-1) * \xi)$. With the introduction of parameters, the solutions of the subproblems can be correlated to avoid updating too fast in a set of optimization variables. Take variables $\mathbf{P}_R$ as an example, with the solution to relay UAV R's power optimization subproblem in $k+1$-th iteration $\tilde{P}_R^{k+1}[n]$, the current solution is set as $P_R^{k+1}[n] = \eta\left(\tilde{P}_R^{k+1}[n] - P_R^k[n]\right) + P_R^k[n]$. The details of the proposed joint trajectory and transmit power optimization algorithm in the cooperative UAV-enabled secure mobile relay scheme are summarized in Algorithm 1.

Here we discuss the convergence of Algorithm 1. In the classical block coordinate descent method, the sub-problem for updating each block of variables is required to be solved exactly with optimality in each iteration in order to guarantee the convergence [31]. However, in our case, for the optimization subproblems (P4), (P5), (P3), and (P2), we only solve their approximate problems (P4.2), (P5.2), (P3'), and (P2') optimally. Thus, the convergence analysis for the classical coordinate descent method cannot be directly applied, and the convergence of Algorithm 1 needs to be proved, as shown below.

Define

$$\begin{aligned}
R_{J,traj}^{lb,k}(\mathbf{Q}_J, \mathbf{Q}_R, \mathbf{P}_J, \mathbf{P}_R) &= R_{J,traj}^k, \\
R_{R,traj}^{lb,k}(\mathbf{Q}_J, \mathbf{Q}_R, \mathbf{P}_J, \mathbf{P}_R) &= R_{R,traj}^k, \\
R_{J,pow}^{lb,k}(\mathbf{Q}_J, \mathbf{Q}_R, \mathbf{P}_J, \mathbf{P}_R) &= R_{J,pow}^k, \\
R_{R,pow}^{lb,k}(\mathbf{Q}_J, \mathbf{Q}_R, \mathbf{P}_J, \mathbf{P}_R) &= R_{R,pow}^k,
\end{aligned}$$

where $R_{J,traj}^k$, $R_{R,traj}^k$, $R_{J,pow}^k$, and $R_{R,pow}^k$ are respectively the objective values of problems (P4.2), (P5.2), (P3'), and (P2') based on $\mathbf{Q}_J$, $\mathbf{Q}_R$, $\mathbf{P}_J$, and $\mathbf{P}_R$. First, in the step 4 of Algorithm 1, it follows that

$$\begin{aligned}
R\left(\mathbf{Q}_J^k, \mathbf{Q}_R^k, \mathbf{P}_J^k, \mathbf{P}_R^k\right) &\overset{(a)}{=} R_{J,traj}^{lb,k}\left(\mathbf{Q}_J^k, \mathbf{Q}_R^k, \mathbf{P}_J^k, \mathbf{P}_R^k\right) \\
&\quad + \sum_{n=1}^{N}\left(W^k[n]\, u^k[n] - X^k[n]\right) \\
&\overset{(b)}{\leq} R_{J,traj}^{lb,k}\left(\mathbf{Q}_J^{k+1}, \mathbf{Q}_R^k, \mathbf{P}_J^k, \mathbf{P}_R^k\right) \\
&\quad + \sum_{n=1}^{N}\left(W^k[n]\, u^k[n] - X^k[n]\right) \\
&\overset{(c)}{\leq} R\left(\mathbf{Q}_J^{k+1}, \mathbf{Q}_R^k, \mathbf{P}_J^k, \mathbf{P}_R^k\right) \qquad (30)
\end{aligned}$$

where (a) holds since the first-order Taylor expansions in (16a), (16b), and (16c) are tight at given local points, respectively, which means that problem (P4.2) at $\mathbf{Q}_J^k$ has the same objective value as that of problem (P4); (b) holds since in step 4 of Algorithm 1 with given $\mathbf{Q}_R^k$, $\mathbf{P}_J^k$, and $\mathbf{P}_R^k$, problem (P4.2) is solved optimally with solution $\mathbf{Q}_J^{k+1}$; (c) holds since the objective value of problem (P4.2) is the lower bound of that of its original problem (P4) at $\mathbf{Q}_J^{k+1}$. The inequality in (30) suggests that although only an approximate optimization problem (P4.2) is solved for obtaining the jammer UAV's trajectory, the objective value of problem (P4) is still non-decreasing after each iteration.

Second, for given $\mathbf{Q}_J^{k+1}$, $\mathbf{P}_J^k$, and $\mathbf{P}_R^k$ in step 5 of Algorithm 1, it follows that

$$\begin{aligned}
R\left(\mathbf{Q}_J^{k+1}, \mathbf{Q}_R^k, \mathbf{P}_J^k, \mathbf{P}_R^k\right) &\overset{(d)}{=} R_{R,traj}^{lb,k}\left(\mathbf{Q}_J^{k+1}, \mathbf{Q}_R^k, \mathbf{P}_J^k, \mathbf{P}_R^k\right) \\
&\overset{(e)}{\leq} R_{R,traj}^{lb,k}\left(\mathbf{Q}_J^{k+1}, \mathbf{Q}_R^{k+1}, \mathbf{P}_J^k, \mathbf{P}_R^k\right) \\
&\overset{(f)}{\leq} R\left(\mathbf{Q}_J^{k+1}, \mathbf{Q}_R^{k+1}, \mathbf{P}_J^k, \mathbf{P}_R^k\right) \qquad (31)
\end{aligned}$$

which can be similarly shown as in (30). In (31), (d) holds since the first-order Taylor expansions in (20), (22), (23), and (27) are tight at given local points, respectively, which means that problem (P5.2) at $\mathbf{Q}_R^k$ has the same objective value as that of problem (P5); (e) holds since in step 5 of Algorithm 1 with given $\mathbf{Q}_J^{k+1}$, $\mathbf{P}_J^k$, and $\mathbf{P}_R^k$, problem (P5.2) is solved optimally with solution $\mathbf{Q}_R^{k+1}$; (c) holds since the objective value of problem (P5.2) is the lower bound of that of its original problem (P5) at $\mathbf{Q}_R^{k+1}$. The inequality in (31) suggests that although only an approximate optimization problem (P5.2) is solved for obtaining the relay UAV's trajectory, the objective value of problem (P5) is still non-decreasing after each iteration. Next, for given $\mathbf{Q}_J^{k+1}$, $\mathbf{Q}_R^{k+1}$, and $\mathbf{P}_R^k$ in step 6 of Algorithm 1, it follows that

$$\begin{aligned}
&R\left(\mathbf{Q}_J^{k+1}, \mathbf{Q}_R^{k+1}, \mathbf{P}_J^k, \mathbf{P}_R^k\right) \\
&\quad = R_{J,pow}^{lb,k}\left(\mathbf{Q}_J^{k+1}, \mathbf{Q}_R^{k+1}, \mathbf{P}_J^k, \mathbf{P}_R^k\right) \\
&\quad \leq R_{J,pow}^{lb,k}\left(\mathbf{Q}_J^{k+1}, \mathbf{Q}_R^{k+1}, \mathbf{P}_J^{k+1}, \mathbf{P}_R^k\right) \\
&\quad \leq R\left(\mathbf{Q}_J^{k+1}, \mathbf{Q}_R^{k+1}, \mathbf{P}_J^{k+1}, \mathbf{P}_R^k\right) \qquad (32)
\end{aligned}$$

which can be similarly shown as in (31). Then, for given $\mathbf{Q}_J^{k+1}$, $\mathbf{Q}_R^{k+1}$, and $\mathbf{P}_J^{k+1}$ in step 7 of Algorithm 1, it follows that

$$\begin{aligned}
&R\left(\mathbf{Q}_J^{k+1}, \mathbf{Q}_R^{k+1}, \mathbf{P}_J^{k+1}, \mathbf{P}_R^k\right) \\
&\quad = R_{R,pow}^{lb,k}\left(\mathbf{Q}_J^{k+1}, \mathbf{Q}_R^{k+1}, \mathbf{P}_J^{k+1}, \mathbf{P}_R^k\right) \\
&\quad \leq R_{R,pow}^{lb,k}\left(\mathbf{Q}_J^{k+1}, \mathbf{Q}_R^{k+1}, \mathbf{P}_J^{k+1}, \mathbf{P}_R^{k+1}\right) \\
&\quad \leq R\left(\mathbf{Q}_J^{k+1}, \mathbf{Q}_R^{k+1}, \mathbf{P}_J^{k+1}, \mathbf{P}_R^{k+1}\right) \qquad (33)
\end{aligned}$$

which can be similarly shown as in (31). Based on (30), (31), (32), and (33), we obtain

$$R\left(\mathbf{Q}_J^k, \mathbf{Q}_R^k, \mathbf{P}_J^k, \mathbf{P}_R^k\right) \leq R\left(\mathbf{Q}_J^{k+1}, \mathbf{Q}_R^{k+1}, \mathbf{P}_J^{k+1}, \mathbf{P}_R^{k+1}\right) \qquad (34)$$

which indicates that the objective value of the problem (P1) is non-decreasing after each iteration k of Algorithm 1. Since the objective value of the problem (P1) is upper bounded by a finite value, the proposed Algorithm 1 is guaranteed

to converge. Simulation results in Section IV show that the proposed algorithm converges quickly for our considered setup.

Furthermore, for the complex NP original problem, the common globally optimal algorithm, such as branch and bound method, has exponential complexity. Since only convex optimization problems need to be solved in each iteration of Algorithm 1, the proposed algorithm has polynomial complexity $\mathcal{O}\left[L_{ite}KN^{7/2}\right]$, [15], [18], [29] where L_{ite} denotes the iteration number of Algorithm 1. Algorithm 1 can be practically implemented with relatively fast convergence for wireless networks containing a moderate number of devices.

IV. SIMULATIONS

In this section, simulations are implemented to validate the effectiveness of our proposed cooperative UAV-enabled secure mobile relaying design. The proposed algorithm performs joint trajectory and transmit power optimization for both the relay UAV and the jammer UAV. Simulations results show the effect of our proposed cooperatively joint trajectory and power optimization scheme (denoted by C-T&P in this section). Besides, we introduce following three benchmark schemes as comparison: joint trajectory and power optimization for single relay UAV without the friendly jammer (denoted by S-NJ), joint trajectory and transmit power optimization for both the relay UAV and the trajectory optimization for the jammer UAV with fixed transmit power (denoted by C-T/NP), and joint optimization for the relay UAV and power control on the jammer UAV with fixed-line-segment trajectory (denoted by C-LT/P). Especially, in S-NJ, we set $\mathbf{P}_j = 0$ and then solved (P2) and (P5) iteratively until convergence, where $\mathbf{P}_j = 0$ represents there is only one UAV, i.e., the relay UAV in this single UAV scheme. In C-T/NP, we solved (P2'), (P4.2), and (P5.2) iteratively in an alternating manner to cooperatively optimize the flight trajectories of the jammer UAV and the relay UAV and transmit power of the relay UAV until convergence. The jammer UAV's transmit power is fixed at the average power $\bar{P}_J$. C-T/NP can be regarded as an incompletely cooperative scheme where the power resource of the jammer is partially limited. In C-LT/P, (P5.2), (P3'), and (P2') are solved iteratively till convergence. The jammer UAV's trajectory is fixed-line-segments connected the initial locations to the final locations. This scheme can be used in a situation where the mobility of the UAV jammer is restricted.

We consider two practical cases where UAVs have different initial and final locations, denoted by Case 1 and Case 2, respectively. In Case 1, two UAVs have adjacent initial/final locations set as $\mathbf{q}_{R0} = [155, 250]^T$ m, $\mathbf{q}_{RF} = [155, -250]^T$ m, $\mathbf{q}_{J0} = [145, 250]^T$ m, and $\mathbf{q}_{JF} = [145, -250]^T$ m. The connecting lines between each UAV's respective initial and final locations are perpendicular to the connecting line between source S and destination D. In Case 2, the respective initial/final locations of both UAVs are on a parallel line of the connecting lines between S and D with the coordinates set as $\mathbf{q}_{R0} = [-100, 0]^T$ m, $\mathbf{q}_{RF} = [400, 0]^T$ m, $\mathbf{q}_{J0} = [-100, -10]^T$ m, $\mathbf{q}_{JF} = [400, -10]^T$ m. In all schemes of two cases, the UAVs' trajectories are initialized by line-segments trajectory connecting their initial locations to final locations respectively, while the power of the UAV is initialized by the average transmit power $\bar{P}_R$ and $\bar{P}_J$ for the relay UAV and the jammer UAV, respectively. Other parameters in the simulations are set as follows: $H = 50$m, $V = 10$m/s, $\delta_t = 1$s, $\mathbf{w}_S = [0, 0]^T$ m, $\mathbf{w}_D = [300, 0]^T$ m, $\mathbf{w}_E = [125, -50]^T$ m, $\gamma_0 = 80$dB, $\bar{P}_R = 10$dBm, $P_{R\max} = 4\bar{P}_R = 16$dBm, $\bar{P}_J = 10$dBm, $P_{J\max} = 4\bar{P}_J = 16$dBm, $P_S = 30$dBm, $\eta = 0.5$, $\xi = 0.08$, and $\varepsilon = 10^{-4}$.

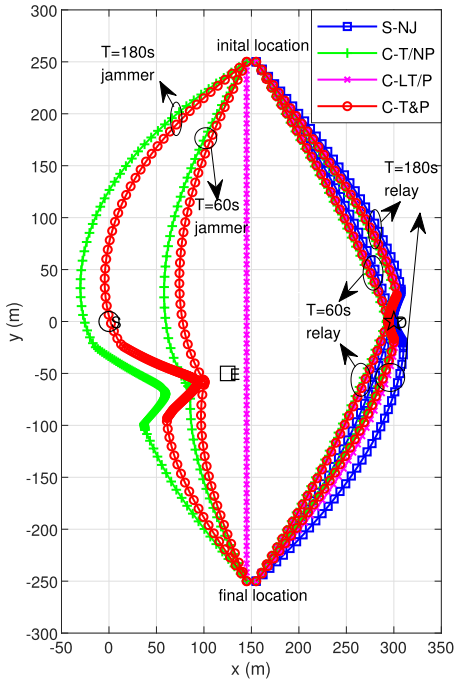

FIGURE 2. Trajectories of the proposed scheme and the benchmark schemes in case 1.

A. SIMULATION RESULTS FOR CASE 1

1) UAVs' TRAJECTORY FOR DIFFERENT SCHEMES

As a common optimizing operation in the UAV-enabled mobile relay system, the relay UAV R's trajectory and transmit power are jointly optimized in all mentioned schemes. In our proposed cooperative jamming scheme, the jammer and the resources on it are the variables to focus on in simulations. For the jammer UAV, trajectory optimization is performed in two schemes: C-T&P and C-T/NP. We demonstrate the trajectories of UAVs for all mentioned schemes with different flight period T in Fig.2. The S (source), D (destination), and E (eavesdropper) are marked in the figure by the circle, star, and square, respectively. It can be drawn that the minimum flight period is $T = 50$s, where UAVs in different schemes fly in similar trajectories from their initial points to the final points straightly at maximum speed. We adopt $T = 60$s and $T = 180$s in our simulations to represent insufficient and sufficient mission time, respectively.

For the simulation results of our proposed scheme C-T&P, the trajectories of two UAVs in Fig.1 can be divided into three stages: 1) both UAVs fly to their quasi-stationary areas at maximum speed; 2) both UAVs fly at low speed in the path near to E or D; 3) both UAVs fly to their final locations at maximum speed. Specifically, in the first stage, the jammer UAV J flies to a point near the eavesdropper E in an arc path while UAV R flies to a point near the destination D. Considering the initial and final locations of UAVs and the location of eavesdropper and destination, two UAVs fly to their quasi-stationary areas submitted to their mission requirements. In the second stage, the jammer UAV flies near the eavesdropper to get a better jamming channel and send as much interference as possible to confuse the eavesdropper. The relay UAV also attempts to relay the confidential information with high throughput. Because the source has much higher transmit power than the relay UAV, the relay therefore flies to the area near the destination to maintain the balance between uplink and downlink communications. Finally, in the third stage, both UAVs need to reserve enough time to fly to the final points at maximum speed.

For the trajectory of relay UAV R, benchmark algorithms C-T/NP, C-LT/P, and S-NJ have the same stages as our proposed algorithm C-T&P. However, from Fig.2, we can observe that the jammer UAV affects the relay UAV's trajectory. The trajectories of C-T/NP and C-LT/P are similar to C-T&P, while the scheme S-NJ experience a longer path during the mission to avoid the eavesdropper. We can also observe that the relay UAV in all schemes have more intensive trajectory points around destination D and fly a farther path at $T = 180$s compared with the results at $T = 60$s, which can be attributed to more elaborate trajectory optimization with sufficient flight time. For the trajectory of jammer UAV J, benefit from joint trajectory and power optimization, the UAV J experience shorter flight distance in C-T&P compared with C-T/NP, which also means energy-efficient flight in practical scenarios. The changes in the jammer UAV's trajectories over flight time T are similar to the previous analysis on the relay UAV.

2) UAVs' POWER FOR DIFFERENT SCHEMES

For case 1, Fig.3 and Fig.4 show the transmit power control of both UAVs in different schemes where $T = 60$s and $T = 180$s, respectively. The initial transmit power for all schemes is set as 10dBm (0.01W). In Fig.3, the transmit power of relay UAV in C-T&P, C-T/NP, and C-LT/P have a similar trend: monotonically decreasing after increasing to a peak. Combined with the flight trajectory, it can be figured out that at the beginning of the mission, the relay UAV does not receive much data from the source. In the process of flying to the information destination, the relay UAV receives and stores a lot of packets. When the relay UAV R is close enough to the information destination D, the achievable rate form R to D significantly exceeds the achievable rate on the eavesdropper wiretapping R, and the transmit power of R reaches the peak.

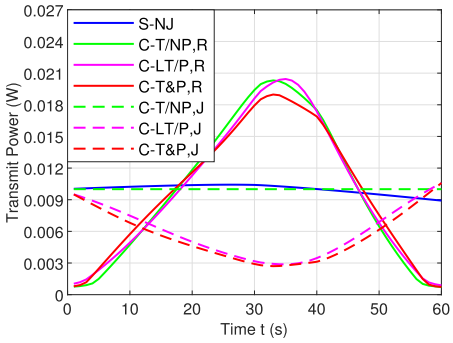

FIGURE 3. Power control of the proposed scheme and the benchmark schemes in case 1 when T=60s.

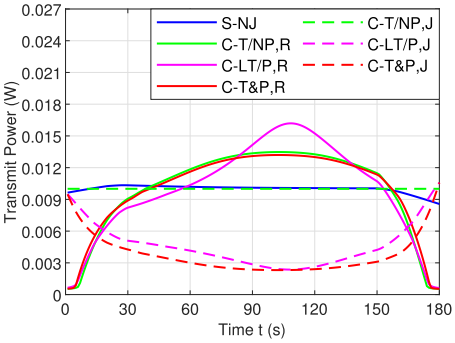

FIGURE 4. Power control of the proposed algorithm and the benchmark algorithms in case 1 when T=180s.

The transmit power curve of scheme S-NJ has relatively small variation compared with the three schemes mentioned above, which is close to the initial power settings. The difference of power control between S-NJ and other schemes shows that the introduction of cooperative jamming UAV can make the resources on the UAV fully optimized.

In C-T&P and C-LT/P, the jammer UAV's transmit power is optimized, and the power curves show the opposite trend to relay UAV's transmit power curve. The jammer UAV keeps transmitting noise to space, and it degrades the achievable rate over the legitimate channel as well, although the eavesdropper is confused by the noise. Thus, when the jammer UAV J approaches the eavesdropper E, the improved channel condition between J and E owing to short distance is utilized by the friendly jammer to combat against the eavesdropper. It is enough to confuse the eavesdropper and reduce the negative influence on the legitimate communication links by using a relatively low transmit power.

When $T = 180$s, we can observe that the trends of both UAVs' transmit power in all schemes are similar with the situation at $T = 60$s. However, there are some differences between the two flight time settings. The peak power of the relay UAV declines considerably in C-T&P and C-TN/P, following up with the more evenly distributed transmit power over the mission, which is because of the limited total power on the UAVs. C-LT/P also has similar changes, but the effect is not obvious compared with the former schemes. It is worth

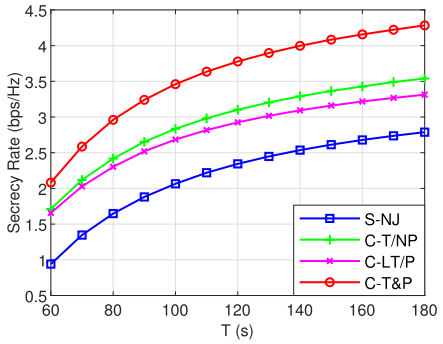

FIGURE 5. Secrecy rate performance for the proposed algorithm and the benchmark algorithms in case 1.

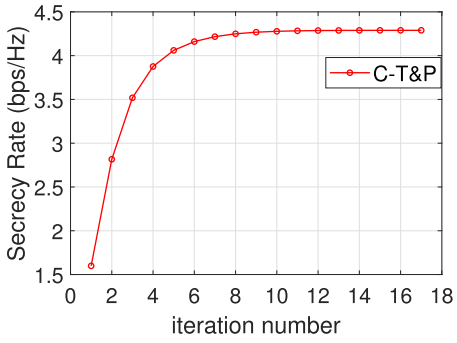

FIGURE 6. Convergence behaviour of the proposed Algorithm 1.

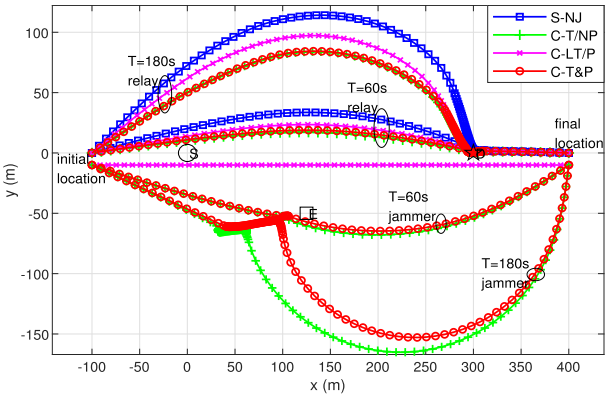

FIGURE 7. Trajectories of the proposed algorithm and the benchmark algorithms in case 2.

mentioning that the lower peak power reduces the requirements on the device.

3) SECRECY RATE PERFORMANCE FOR MENTIONED SCHEMES

Our objective is maximizing the average achievable secrecy rate in the UAV-enabled relay systems. Fig.5 demonstrates the average secrecy rate versus the different flight duration T for different schemes. From Fig.5, we can observe that the average secrecy rate raised monotonously as the flight period T increases for all schemes. This result can be attributed to the extra optimization freedom brought by more flight time. It can be shown that there is a relatively steady performance improvement in C-T&P compared with other benchmark schemes.

Especially, our proposed scheme significantly outperforms the single UAV relay system, which verifies the effectiveness of our proposed cooperation scheme. The introduction of a friendly UAV jammer to the UAV-enabled relay system improves system performance effectively in case 1. Besides, compared with joint trajectory and power optimization for the UAV jammer, there is certain performance degradation when the resources on the UAV are limited, i.e., trajectory optimization without power control or power optimization with fixed trajectory.

4) CONVERGENCE BEHAVIOUR OF THE PROPOSED ALGORITHM

The convergence behavior of the proposed Algorithm 1 is shown in Fig.6 in case 1 under $T = 180$s. It can be observed from Fig.6 that the average achievable secrecy rate increases quickly with the number of iterations, and the algorithm converges in about 17 iterations.

B. SIMULATION RESULTS FOR CASE 2

1) UAVs' TRAJECTORY FOR MENTIONED SCHEMES

In this section, we consider case 2 with different UAVs' initial and final locations settings compared to case 1. The UAVs' trajectories for all schemes in two fight periods $T = 60$s and $T = 180$s are shown in Fig.7. The trajectories for the jammer UAV and the relay UAV in our proposed scheme can be divided into three stages, respectively. In the first stage, the relay UAV flies towards information destination D in an arc path at maximum speed and then reduce speed when close to D. At the same time, the jammer UAV flies towards the eavesdropper E and reduce their speed around E to combat against it. The reason behind the arc path is that two UAVs attempt to minimize the interference on the relay UAV transmitted by the friendly jammer and the relay UAV can fly away from the eavesdropper as well. In the second stage, the jammer UAV flies at low speed around the eavesdropper and the relay UAV flies around D slowly. This stage is similar to that in case 1. In the third stage, the relay UAV flies straightly to the final location while the jammer UAV still flies in an arc path towards the final location to reduce the inference to the destination D and the relay UAV.

The trajectories of the relay UAVs in the other three benchmark schemes are similar to our proposed scheme with longer flight distance. The single UAV in S-NJ has the longest flight distance in all relay UAVs. From a fight time perspective, UAVs under $T = 180$s also have longer flight path and fly more outside towards each other than UAVs under $T = 60$s owing to the sufficient flight time.

2) UAVs' TRANSMIT POWER FOR MENTIONED SCHEMES

For case 2, Fig.8 and Fig.9 show the transmit power of UAVs in different schemes where $T = 60$s and $T = 180$s,

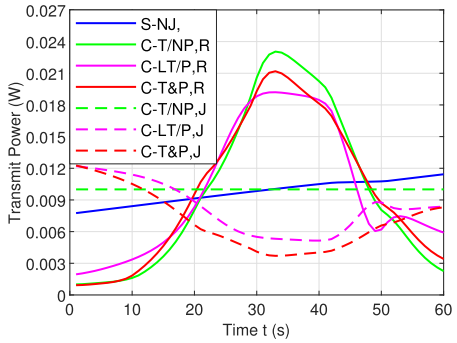

FIGURE 8. Power control of the proposed algorithm and the benchmark algorithms in case 2 when T=60s.

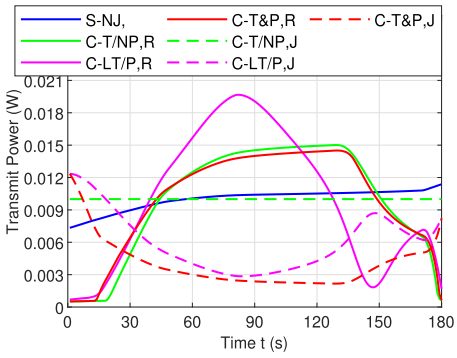

FIGURE 9. Power control of the proposed algorithm and the benchmark algorithms in case 2 when T=180s.

respectively. The transmit power of the jammer UAV in C-LT/P maintains initial power 0.01W as a reference. In S-NJ, the relay UAV's power monotonous increase with a slight change. The power curves of the relay UAV in C-T/NP and C-T&P increase until reaching the peak power and then decrease though the curve is not very smooth. The peak power reduces in a larger flight period. Affected by limited trajectory resource, the power in C-LT/P has a certain fluctuation at the end of the flight. From the perspective of the average power of each UAV, our proposed scheme is energy-efficient compared to the schemes contained two UAVs.

3) SECRECY RATE PERFORMANCE FOR MENTIONED SCHEMES

Fig.10 plots average achievable secrecy rate performance versus the flight period T in case 2 for all schemes. Three benchmark schemes show different results compared with performance curves in case 1, Fig.5. The average achievable secrecy rate raises over the increase of T. The secrecy rates of C-LT/P are lower than the other schemes include single UAV scheme S-NJ, which can be attributed to limited trajectory resources on the jammer UAV in case 2. The limited trajectory of the jammer UAV leads to additional interference on the relay UAV R and the information destination D brought by J. The performance degradation in C-LT/P shows the importance of trajectory optimization in cooperative

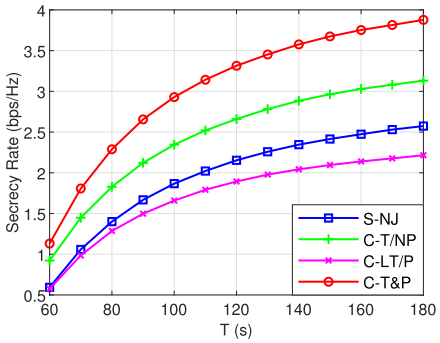

FIGURE 10. Secrecy rate performance of the proposed algorithm and the benchmark algorithms in case 2.

schemes. Our proposed scheme C-T&P and another benchmark scheme C-T/NP maintain a stable performance gap over all Ts compared to the other two schemes. Cooperative scheme C-T/NP without power control on the jammer UAV still brings benefits. However, by performing joint transmit power and trajectory optimization on both UAVs cooperatively, our proposed scheme C-T&P significantly outperforms the other three benchmark schemes over any flight period T. The average achievable secrecy rate in a UAV-enabled relay system can be enhanced by introducing a cooperative jammer UAV and jointly optimizing both UAV's resources. The simulation results in case 2 validate the effectiveness of our proposed scheme once again. Besides, compared to the curves in Fig.10, Fig.5 shows that the average achievable secrecy rates in our proposed scheme over all flight time in case 1 are higher than that in case 2. This difference enlightens us that the UAV's initial and final locations need to be taken into consideration in future works to obtain better performance.

V. CONCLUSION

This paper studies the physical-layer security issue in a UAV-enabled mobile relay system with a terrestrial eavesdropper. A cooperative UAV jammer is employed to combat against the eavesdropper and improve the security performance of the system. The secrecy rate maximization problem is formulated to maximize the average achievable secrecy rate over a given flight period, subject to transmit power constraints and practical mobility constraints on both UAVs along with the information-causality constraint on the relay UAV. The non-convex original problem is decoupled into to four tractable subproblems. By applying update-rate-assisted block coordinate descent and successive convex optimization techniques, an efficient iterative algorithm is then proposed to solve the subproblems alternatively in an iterative manner. Though the proposed algorithm tends to converge to local optimum, it has polynomial complexity, which can be practically implemented with relatively fast convergence. Numerical results show that our proposed cooperative scheme with joint trajectory and transmit power optimization on the UAVs significantly outperforms three benchmark schemes.

Our proposed scheme provides new insights into security issues in the UAV-enabled mobile relay system. The results in this paper can be further extended for the case with only imperfect knowledge of eavesdropper's location. The proposed scheme can also serve as the basis for secure mobile relay systems with multiple UAVs or multiple eavesdroppers. Besides, in our future work, the tradeoff between performance and consumption should be taken into account, and the energy-efficient secure relaying scheme will be considered.

REFERENCES

[1] J. Lyu, Y. Zeng, R. Zhang, and T. J. Lim, "Placement optimization of UAV-mounted mobile base stations," *IEEE Commun. Lett.*, vol. 21, no. 3, pp. 604–607, Mar. 2017.

[2] Y. Zeng and R. Zhang, "Energy-efficient UAV communication with trajectory optimization," *IEEE Trans. Wireless Commun.*, vol. 16, no. 6, pp. 3747–3760, Jun. 2017.

[3] Q. Wu, Y. Zeng, and R. Zhang, "Joint trajectory and communication design for multi-UAV enabled wireless networks," *IEEE Trans. Wireless Commun.*, vol. 17, no. 3, pp. 2109–2121, Mar. 2018.

[4] Y. Zeng, X. Xu, and R. Zhang, "Trajectory design for completion time minimization in UAV-enabled multicasting," *IEEE Trans. Wireless Commun.*, vol. 17, no. 4, pp. 2233–2246, Apr. 2018.

[5] Y. Zeng, R. Zhang, and T. J. Lim, "Throughput maximization for UAV-enabled mobile relaying systems," *IEEE Trans. Commun.*, vol. 64, no. 12, pp. 4983–4996, Dec. 2016.

[6] Y. Chen, W. Feng, and G. Zheng, "Optimum placement of UAV as relays," *IEEE Commun. Lett.*, vol. 22, no. 2, pp. 248–251, Feb. 2018.

[7] S. Zhang, H. Zhang, Q. He, K. Bian, and L. Song, "Joint trajectory and power optimization for UAV relay networks," *IEEE Commun. Lett.*, vol. 22, no. 1, pp. 161–164, Jan. 2018.

[8] Y. Chen, N. Zhao, Z. Ding, and M.-S. Alouini, "Multiple UAVs as relays: Multi-hop single link versus multiple dual-hop links," *IEEE Trans. Wireless Commun.*, vol. 17, no. 9, pp. 6348–6359, Sep. 2018.

[9] Q. Zhang, M. Jiang, Z. Feng, W. Li, W. Zhang, and M. Pan, "IoT enabled UAV: Network architecture and routing algorithm," *IEEE Internet Things J.*, vol. 6, no. 2, pp. 3727–3742, Apr. 2019.

[10] M. Gapeyenko, V. Petrov, D. Moltchanov, S. Andreev, N. Himayat, and Y. Koucheryavy, "Flexible and reliable UAV-assisted backhaul operation in 5G mmWave cellular networks," *IEEE J. Sel. Areas Commun.*, vol. 36, no. 11, pp. 2486–2496, Nov. 2018.

[11] S. Zhang, H. Zhang, B. Di, and L. Song, "Cellular UAV-to-X communications: Design and optimization for multi-UAV networks," *IEEE Trans. Wireless Commun.*, vol. 18, no. 2, pp. 1346–1359, Feb. 2019.

[12] C. Zhan, Y. Zeng, and R. Zhang, "Energy-efficient data collection in UAV enabled wireless sensor network," *IEEE Wireless Commun. Lett.*, vol. 7, no. 3, pp. 328–331, Jun. 2018.

[13] Q. Wu, W. Mei, and R. Zhang, "Safeguarding wireless network with UAVs: A physical layer security perspective," *IEEE Wireless Commun.*, vol. 26, no. 5, pp. 12–18, Oct. 2019.

[14] G. Zhang, Q. Wu, M. Cui, and R. Zhang, "Securing UAV communications via trajectory optimization," in *Proc. IEEE Global Commun. Conf. (GLOBECOM)*, Singapore, Dec. 2017, pp. 1–6.

[15] A. Li, Q. Wu, and R. Zhang, "UAV-enabled cooperative jamming for improving secrecy of ground wiretap channel," *IEEE Wireless Commun. Lett.*, vol. 8, no. 1, pp. 181–184, Feb. 2019.

[16] X. Zhou, Q. Wu, S. Yan, F. Shu, and J. Li, "UAV-enabled secure communications: Joint trajectory and transmit power optimization," *IEEE Trans. Veh. Technol.*, vol. 68, no. 4, pp. 4069–4073, Apr. 2019.

[17] Z. Li, M. Chen, C. Pan, N. Huang, Z. Yang, and A. Nallanathan, "Joint trajectory and communication design for secure UAV networks," *IEEE Commun. Lett.*, vol. 23, no. 4, pp. 636–639, Apr. 2019.

[18] Y. Li, R. Zhang, J. Zhang, S. Gao, and L. Yang, "Cooperative jamming for secure UAV communications with partial eavesdropper information," *IEEE Access*, vol. 7, pp. 94593–94603, 2019.

[19] L. Shen, N. Wang, X. Ji, X. Mu, and L. Cai, "Iterative trajectory optimization for physical-layer secure buffer-aided UAV mobile relaying," *Sensors*, vol. 19, no. 15, pp. 3442–3457, 2019.

[20] Q. Wang, Z. Chen, H. Li, and S. Li, "Joint power and trajectory design for physical-layer secrecy in the UAV-aided mobile relaying system," *IEEE Access*, vol. 6, pp. 62849–62855, 2018.

[21] J. Huang and A. L. Swindlehurst, "Buffer-aided relaying for two-hop secure communication," *IEEE Trans. Wireless Commun.*, vol. 14, no. 1, pp. 152–164, Jan. 2015.

[22] D. Yang, Q. Wu, Y. Zeng, and R. Zhang, "Energy tradeoff in ground-to-UAV communication via trajectory design," *IEEE Trans. Veh. Technol.*, vol. 67, no. 7, pp. 6721–6726, Jul. 2018.

[23] J. Zhang, Y. Zeng, and R. Zhang, "UAV-enabled radio access network: Multi-mode communication and trajectory design," *IEEE Trans. Signal Process.*, vol. 66, no. 20, pp. 5269–5284, Oct. 2018.

[24] D. W. Matolak and R. Sun, "Unmanned aircraft systems: Air-ground channel characterization for future applications," *IEEE Veh. Technol. Mag.*, vol. 10, no. 2, pp. 79–85, Jun. 2015.

[25] D. W. Matolak and R. Sun, "Air–ground channel characterization for unmanned aircraft systems—Part I: Methods, measurements, and models for over-water settings," *IEEE Trans. Veh. Technol.*, vol. 66, no. 1, pp. 26–44, Jan. 2017.

[26] *Enhanced LTE Support for Aerial Vehicles*, Sophia Antipolis, France, document Rep. TR 36.777. 3GPP. Accessed: Jul. 16, 2017. [Online]. Available: http://www.3gpp.org/specs/archive/36_series/36.777

[27] Q. Wu and R. Zhang, "Common throughput maximization in UAV-enabled OFDMA systems with delay consideration," *IEEE Trans. Commun.*, vol. 66, no. 12, pp. 6614–6627, Dec. 2018.

[28] P. K. Gopala, L. Lai, and H. El Gamal, "On the secrecy capacity of fading channels," *IEEE Trans. Inf. Theory*, vol. 54, no. 10, pp. 4687–4698, Oct. 2008.

[29] S. Boyd and L. Vandenberghe, *Convex Optimization*. Cambridge, U.K.: Cambridge Univ. Press, 2004.

[30] M. Grant and S. Boyd. (2016). *CVX: MATLAB Software for Disciplined Convex Programming*. [Online]. Available: http://cvxr.com/cvx

[31] D. P. Bertsekas, *Nonlinear Programming*. Belmont, MA, USA: Athena Scientific, 1999.

JIANSONG MIAO received the B.Eng. degree in communication engineering from Jilin University, in 2001, and the Ph.D. degree in communication and information system from the Beijing University of Posts and Telecommunications. As a main Researcher, he has participated in a number of national, provincial and ministerial, and cooperative scientific research projects. He has published over 20 articles. His current research interests include broadband wireless access networks, UAV-assisted communication systems, and mobile adhoc networks.

ZIYUAN ZHENG was born in Beijing, China, in 1996. He received the B.Eng. degree in communication engineering from the Beijing University of Posts and Telecommunications (BUPT), in 2018, where he is currently pursuing the master's degree. His current research interests include unmanned aerial vehicle communications, transceiver optimization for wireless systems, physical layer security, and UAV-assisted communication systems.